3728 *Organometallics* **1999,** *18,* 3728−3736

Synthesis and Structures of Two Isomeric Pairs of Tetrathiotungstate Clusters, $[\{Cp^*Ru(CO)\}_2(WS_4)\{W(CO)_4\}]$ and $[\{Cp^*Ru(CO)\}_2(WS_4)]$ ($Cp^* = \eta^5\text{-}C_5Me_5$), by Reaction of $[Cp^*_2Ru_2S_4]$ with $[W(CO)_3(NCMe)_3]$

Masahiro Yuki, Masaaki Okazaki, Shinji Inomata, and Hiroshi Ogino*

Department of Chemistry, Graduate School of Science, Tohoku University, Sendai 980-8578, Japan

Received June 7, 1999

An isomeric pair of tetranuclear clusters containing tetrathiotungstate $[WS_4]^{2-}$, $[\{Cp^*Ru(CO)\}_2\{W(\mu_3\text{-}S)_2(\mu_2\text{-}S)_2\}\{W(CO)_4\}]$ (**1a**) and $[\{Cp^*Ru(CO)\}_2\{W(\mu_3\text{-}S)_3({=}S)\}\{W(CO)_4\}]$ (**2a**) ($Cp^* = \eta^5\text{-}C_5Me_5$), and the trinuclear cluster $[\{Cp^*Ru(CO)\}_2\{W(\mu_3\text{-}S)(\mu_2\text{-}S)_2({=}S)\}]$ (**3a**) were formed upon thermal reaction of $[Cp^*_2Ru_2S_4]$ with 2 equiv of $[W(CO)_3(NCMe)_3]$. In the course of the reaction, redistribution of CO and S ligands took place between Ru and W atoms without losing any CO and S ligands. When the reaction was performed with 1 equiv of $[W(CO)_3(NCMe)_3]$, **2a** and the trinuclear cluster $[\{Cp^*Ru(CO)\}_2\{W(\mu_2\text{-}S)_4\}]$ (**5a**), which is the isomer of **3a**, were obtained. Trinuclear clusters **3a** and **5a** were converted to tetranuclear clusters **1a** and **2a** by the reaction with $[W(CO)_3(NCMe)_3]$ and CO. Thus, the trinuclear clusters **3a** and **5a** were considered to be intermediates to give the tetranuclear clusters **1a** and **2a**.

Introduction

Dinuclear transition-metal sulfide complexes $[Cp^{\#}_2M_2S_4]$ ($Cp^{\#}$ = cyclopentadienyl (Cp) and substituted-Cp ligands) have been explored as good precursors in the synthesis of organometallic sulfide clusters.[1] For instance, Rauchfuss et al. have reported a variety of sulfide clusters containing late transition metals such as Fe, Co, Ni, and Ir by using $[(\eta^5\text{-}C_5H_4Me)_2V_2S_4]$.[2] Recently, our group reported that the reactions of $[Cp^*_2Fe_2S_4]$ ($Cp^* = \eta^5\text{-}C_5Me_5$) with Fe and Ru carbonyls afforded *closo*-$[Cp^*_2Fe_2MS_2(CO)_3]$ clusters (M = Fe, Ru).[3] For the ruthenium analogue, the reactions of $[Cp^*_2Ru_2S_4]$ with $[Cp^*Ru(NCMe)_3](PF_6)$, $[CpRu(NCMe)_3](PF_6)$, and $[Cp^*Rh(NCMe)_3](PF_6)_2$ gave $[Cp^*_3Ru_3S_4](PF_6)$,[4a] $[Cp^*_2Cp_2Ru_4S_4](PF_6)_2$,[4b] and $[Cp^*_3RhRu_2S_4(NCMe)](PF_6)_2$,[4c] respectively. In contrast, few studies have been carried out on the reactions of $[Cp^{\#}_2M_2S_4]$ with early-transition-metal complexes.[5] This paper describes cluster construction by the reaction of $[Cp^*_2Ru_2S_4]$ with $[W(CO)_3(NCMe)_3]$, which was carried out at 50 °C to give an isomeric pair of tetranuclear clusters, $[\{Cp^*Ru(CO)\}_2\{W(\mu_3\text{-}S)_2(\mu\text{-}S)_2\}\{W(CO)_4\}]$ (**1a**) and $[\{Cp^*Ru(CO)\}_2\{W(\mu_3{-}S)_3({=}S)\}\{W(CO)_4\}]$ (**2a**). Plausible reaction pathways to the tetranuclear clusters **1a** and **2a** which involve the transient formation of an isomeric pair of trinuclear clusters, $[\{Cp^*Ru(CO)\}_2\{W(\mu_3{-}S)(\mu\text{-}S)_2({=}S)\}]$ (**3a**) and $[\{Cp^*Ru(CO)\}_2\{W(\mu_3{-}S)_2(\mu\text{-}S)_2\}]$ (**5a**), are proposed. Characterization and some properties of **3a** and **5a** are also described. Part of this work has been previously reported in a preliminary form.[6]

Results and Discussion

Reaction of $[Cp^*_2Ru_2S_4]$ with 2 Equiv of $[W(CO)_3(NCMe)_3]$. To an acetonitrile solution of 2 equiv of $[W(CO)_3(NCMe)_3]$ was added a toluene solution of $[Cp^*_2Ru_2S_4]$ (eq 1). Heating the mixture at 50 °C for 40 min produced two kinds of $Ru_2W_2S_4$ clusters, **1a** and **2a**, and

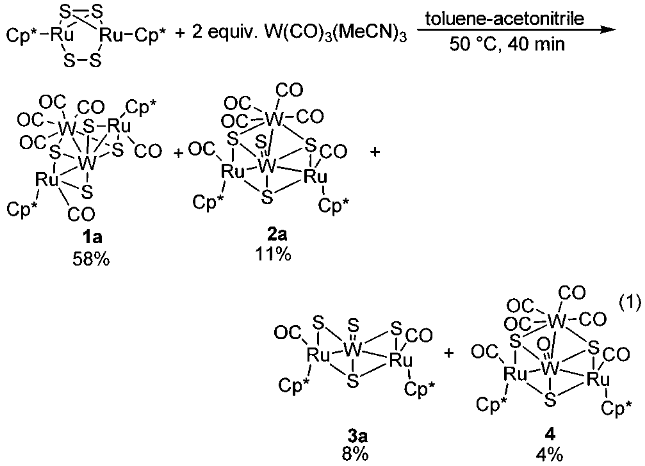

---

[1] Wachter, J. *Angew. Chem., Int. Ed. Engl.* **1989**, *28*, 1613 and references therein.

[2] (a) Rauchfuss, T. B.; Weatherill, T. D.; Wilson, S. R.; Zebrowski, J. P. *J. Am. Chem. Soc.* **1983**, *105*, 6508. (b) Bolinger, C. M.; Weatherill, T. D.; Rauchfuss, T. B.; Rheingold, A. L.; Day, C. S.; Wilson, S. R. *Inorg. Chem.* **1986**, *25*, 634. (c) Rauchfuss, T. B.; Gammon, S. D.; Weatherill, T. D.; Wilson, S. R. *New J. Chem.* **1988**, *12*, 373.

[3] Mitsui, T.; Inomata, S.; Ogino, H. *Inorg. Chem.* **1994**, *33*, 4934.

[4] (a) Houser, E. J.; Krautscheid, H.; Rauchfuss, T. B.; Wilson, S. R. *J. Chem. Soc., Chem. Commun.* **1994**, 1283. (b) Feng, Q.; Rauchfuss, T. B.; Wilson, S. R. *J. Am. Chem. Soc.* **1995**, *117*, 4702. (c) Veturelli, A.; Rauchfuss, T. B.; Verma, A. K. *Inorg. Chem.* **1997**, *36*, 1360.

[5] (a) Brunner, H.; Kauermann, H.; Meier, W.; Wachter, J. *J. Organomet. Chem.* **1984**, *263*, 183. (b) Brunner, H.; Kauermann, H.; Wachter, J. *J. Organomet. Chem.* **1984**, *265*, 189. (c) Brunner, H.; Kauermann, H.; Pfauntsch, J.; Wachter, J. *J. Organomet. Chem.* **1987**, *331*, 45.

10.1021/om990432m CCC: $18.00

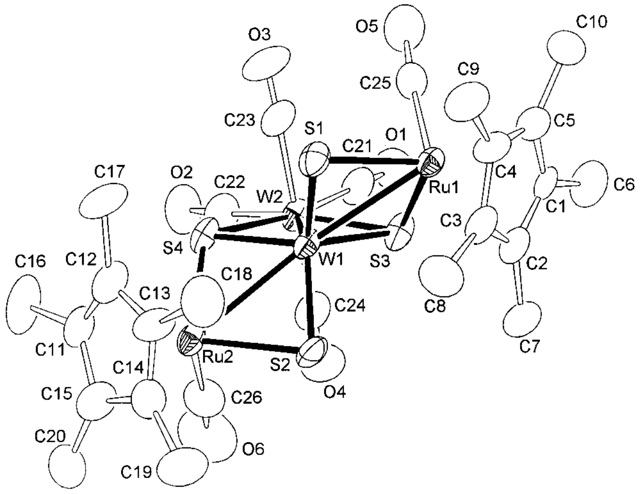

Figure 1. ORTEP drawing of $[\{Cp^*Ru(CO)\}_2\{W(\mu_3\text{-}S)_2(\mu\text{-}S)_2\}\{W(CO)_4\}]$ (**1a**) with 50% ellipsoids.

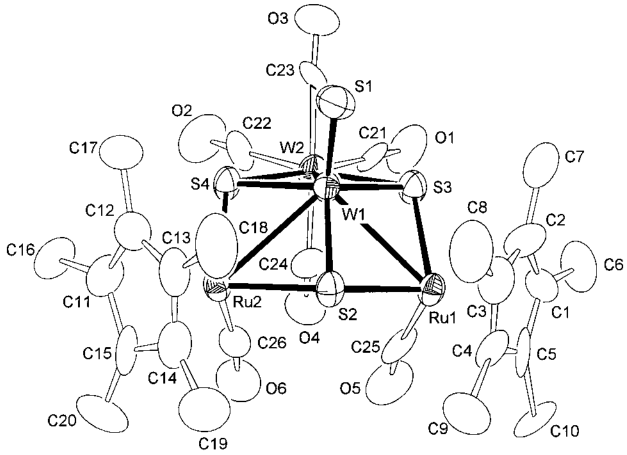

Figure 2. ORTEP drawing of $[\{Cp^*Ru(CO)\}_2\{W(\mu_3\text{-}S)_3(=S)\}\{W(CO)_4\}]$ (**2a**) with 50% ellipsoids.

Table 1. Selected Interatomic Distances (Å) and Bond Angles (deg) for $[\{Cp^*Ru(CO)\}_2\{W(\mu_3\text{-}S)_2(\mu\text{-}S)_2\}\{W(CO)_4\}]$ (1a)

W1−W2	2.9053(7)	W2−S4	2.553(3)
W1−Ru1	2.874(2)	Ru1−S1	2.403(4)
W1−Ru2	2.869(2)	Ru1−S3	2.387(3)
W1−S1	2.212(3)	Ru2−S2	2.395(3)
W1−S2	2.196(3)	Ru2−S4	2.384(4)
W1−S3	2.268(4)	O3···O5	3.18(2)
W1−S4	2.272(3)	O4···O6	3.19(2)
W2−S3	2.551(3)		
W2−W1−Ru1	98.82(3)	S3−W1−S4	115.0(1)
W2−W1−Ru2	98.98(3)	S3−W2−S4	97.2(1)
Ru1−W1−Ru2	162.08(4)	S3−W2−C22	172.8(5)
S1−W1−S2	111.8(1)	S3−W2−C23	98.3(4)
S1−W1−S3	106.5(1)	S4−W2−C21	170.7(4)
S1−W1−S4	109.1(1)	S4−W2−C23	83.2(5)
S2−W1−S3	107.6(1)	C23−W2−C24	176.8(5)
S2−W1−S4	106.9(1)		

Table 2. Selected Interatomic Distances (Å) and Bond Angles (deg) for $[\{Cp^*Ru(CO)\}_2\{W(\mu_3\text{-}S)_3(=S)\}\{W(CO)_4\}]\cdot 2CH_2Cl_2$ ($2a\cdot 2CH_2Cl_2$)

W1−W2	2.997(1)	W2−S4	2.566(6)
W1−Ru1	2.900(2)	Ru1−S2	2.394(6)
W1−Ru2	2.892(2)	Ru1−S3	2.421(6)
W1−S1	2.125(7)	Ru2−S2	2.373(6)
W1−S2	2.261(6)	Ru2−S4	2.408(6)
W1−S3	2.274(6)	O4···O5	3.07(3)
W1−S4	2.276(5)	O4···O6	3.09(3)
W2−S3	2.558(6)	O5···O6	3.14(3)
W2−W1−Ru1	95.45(5)	S3−W1−S4	112.0(2)
W2−W1−Ru2	95.69(5)	S3−W2−S	494.8(2)
Ru1−W1−Ru2	94.55(6)	S4−W2−C21	176.5(7)
S1−W1−S2	109.9(2)	S3−W2−C22	174.8(9)
S1−W1−S3	110.2(3)	S3−W2−C23	89.8(7)
S1−W1−S4	110.4(3)	S4−W2−C23	87.4(6)
S2−W1−S3	107.4(2)	C23−W2−C24	170(1)
S2−W1−S4	106.8(2)		

the Ru_2WS_4 cluster **3a**. A small amount of the $Ru_2W_2S_3O$ cluster **4** was also obtained. The oxygen atom of the terminal oxide in cluster **4** may be derived from O_2 or H_2O as an impurity. Elemental analysis and mass spectral data indicated that **1a** and **2a** have the identical formula $Cp^*_2Ru_2W_2S_4(CO)_6$.[7] Spectroscopic features of **1a** are quite similar to those of **2a**. The ^1H NMR spectra of **1a** and **2a** established that two Cp* ligands in each complex are chemically equivalent. The IR spectra of **1a** and **2a** exhibit strong bands in the terminal CO stretching vibration region and no band in the bridging CO region. The C_5Me_4Et analogues **1b**, **2b,** and **3b** were also obtained by a procedure similar to eq 1.

Clusters **1a** and **2a** were characterized by a single-crystal X-ray diffraction analysis. The ORTEP drawings of **1a** and **2a** are shown in Figures1 and 2, respectively. Selected interatomic distances and bond angles of **1a** and **2a** are given in Tables1 and 2, respectively. Each cluster contains a $[WS_4]^{2-}$ moiety which acts as a bridging ligand and connects one $W(CO)_4$ and two Cp*Ru(CO) fragments. In the reaction, the redistribution of S and CO ligands occurred between two Ru and two W atoms without losing any S and CO ligands. In cluster **1a**, the W1 atom with four S ligands adopts a slightly distorted tetrahedral geometry with S−W−S angles of 106.5(1)−115.0(1)°. The WS_4 fragment is bound to one W by two S atoms and two Ru atoms by four S atoms, two of which bridge one Ru and two W atoms in a μ_3-fashion and the other two bind to one Ru and one W atom in a μ_2-fashion. The W2 atom with four carbonyl ligands and two S ligands adopts a distorted octahedral geometry. The three metal−metal distances of W1−W2 (2.9053(7) Å), W1−Ru1 (2.874(2) Å), and W1−Ru2 (2.869(2) Å) lie in the normal range expected for metal−metal single bonds.[8,9] The W−S distances in $[WS_4]^{2-}$ at 2.196(3)−2.272(3) Å are similar to those in tetrathiotungstate clusters previously reported, which

---

(6) Yuki, M.; Okazaki, M.; Inomata, S.; Ogino, H. *Angew. Chem., Int. Ed.* **1998**, *37*, 2126.

(7) A few isomeric pairs of sulfur clusters have been reported: (a) Braunstein, P.; Jud, J. M.; Tiripicchio, A.; Tiripicchio-Camellini, M.; Sappa, E. *Angew. Chem., Int. Ed. Engl.* **1982**, *21*, 307. (b) Williams, P. D.; Curtis, M. D.; Duffy, D. N.; Butler, W. M. *Organometallics* **1983**, *2*, 165.

(8) (a) Hanewald, K.; Kiel, G.; Gattow, G. *Z. Anorg. Allg. Chem.* **1981**, *478*, 215. (b) Secheresse, F.; Lefebvre, J.; Daran, J. C.; Jeannin, Y. *Inorg. Chem.* **1982**, *21*, 1311. (c) Müller, A.; Hellmann, W.; Römer, C.; Römer, M.; Bögge, H.; Jostes, R.; Schimanski, U. *Inorg. Chim. Acta* **1984**, *83*, L75. (d) Wardle, R. W. M.; Bhaduri, S.; Chau, C.-N.; Ibers, J. A. *Inorg. Chem.* **1988**, *27*, 1747. (e) Hou, Z.; Ozawa, Y.; Isobe, K. *Chem. Lett.* **1990**, 1863. (f) Zhuang, B.; Yu, P.; Huang, L.; He, L.; Lu, J. *Inorg. Chim. Acta* **1990**, *177*, 239.

(9) (a) Howard, K. E.; Rauchfuss, T. B.; Wilson, S. R. *Inorg. Chem.* **1988**, *27*, 1710. (b) Greaney, M. A.; Coyle, C. L.; Harmer, M. A.; Jordan, A.; Stiefel, E. I. *Inorg. Chem.* **1989**, *28*, 912. (c) Howard, K. E.; Lockemeyer, J. R.; Massa, M. A.; Rauchfuss, T. B.; Wilson, S. R.; Yang, X. *Inorg. Chem.* **1990**, *29*, 4385. (d) Kato, M.; Kawano, M.; Taniguchi, H.; Funaki, M.; Moriyama, H.; Sato, T.; Matsumoto, K. *Inorg. Chem.* **1992**, *31*, 26. (e) Mizobe, Y.; Hosomizu, M.; Kubota, Y.; Hidai, M. *J. Organomet. Chem.* **1996**, *507*, 179.

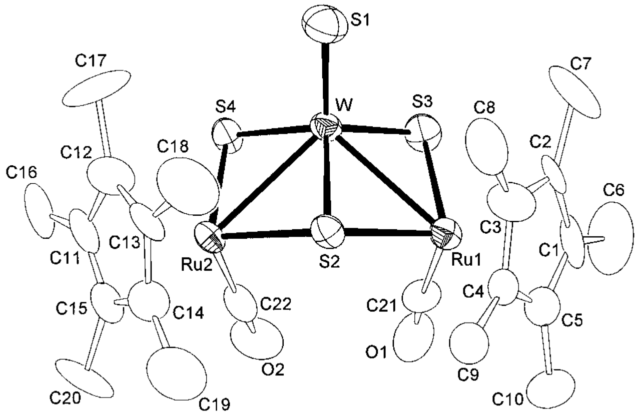

Figure 3. ORTEP drawing of [{Cp*Ru(CO)}$_2${W(μ_3-S)(μ-S)$_2$(=S)}{W(CO)$_4$}] (**3a**) with 50% ellipsoids.

Table 3. Selected Interatomic Distances (Å) and Bond Angles (deg) for [{Cp*Ru(CO)}$_2${W(μ_3-S)(μ-S)$_2$(=S)}] (3a)

W–Ru1	2.890(2)	Ru1–S2	2.368(7)
W–Ru2	2.895(2)	Ru1–S3	2.417(6)
W–S1	2.139(8)	Ru2–S2	2.362(6)
W–S2	2.260(6)	Ru2–S4	2.405(6)
W–S3	2.228(8)	O1···O2	3.02(3)
W–S4	2.238(6)		
Ru1–W–Ru2	94.23(6)	S2–W–S3	107.0(2)
S1–W–S2	110.9(3)	S2–W–S4	106.5(2)
S1–W–S3	111.1(3)	S3–W–S4	110.5(3)
S1–W–S4	110.7(3)		

indicates unsaturated character for the W–S bonds.[10] In contrast, the bond distances of two μ_3-S atoms (S3, S4) to the octahedral W2 atom (2.551(3), 2.553(3) Å) are longer than those of these S atoms to the tetrahedral W1 atom (W1–S3 = 2.268(4) Å, W1–S4 = 2.272(3) Å). It reflects the dative bond character of the former distances. Unlike cluster **1a**, there is a terminal S ligand in **2a**. The WS$_4$ fragment is bound to one W atom by two S atoms and two Ru atoms by three S atoms, two of which bridge one Ru and two W atoms in a μ_3-fashion and the other one binds to two Ru and one W atom in a μ_3-fashion. The three metal–metal bond distances W1–W2 (2.997(1) Å), W1–Ru1 (2.900(2) Å), and W1–Ru2 (2.892(2) Å) are somewhat longer than those of **1a**. The elongation of the metal–metal bonds is attributable to the steric repulsion between CO ligands on Ru1, Ru2, and W2 atoms in cluster **2a** (O4···O5 = 3.07(3) Å, O4···O6 = 3.09(3) Å, O5···O6 = 3.14(3) Å).

Elemental analysis and mass spectral data of **3a** established the formula as Cp*$_2$Ru$_2$WS$_4$(CO)$_2$. The crystal structure of **3a** is shown in Figure 3, and the selected interatomic distances and bond angles of **3a** are listed in Table 3. The structure of **3a** is similar to that of **2a**, except that **3a** has no W(CO)$_4$ moiety. The [WS$_4$]$^{2-}$ fragment is bound to two Ru atoms by three S atoms, two of which bridge one W and one Ru atom in a μ_2-fashion and the other one bridges one W and two Ru atoms in a μ_3-fashion. The residual S atom is bound to the W atom in a terminal mode. Cluster **3a** has a pseudo mirror plane composed of S1, S2, and W atoms. The interatomic distances of W–Ru1 (2.890(2) Å) and W–Ru2 (2.895(2) Å) are within the normal range of metal–metal single-bond distances.[8,9] As in **2a**, there is a steric repulsion between carbonyl ligands of Ru1 and Ru2 metals (O1···O2 = 3.02(3) Å).

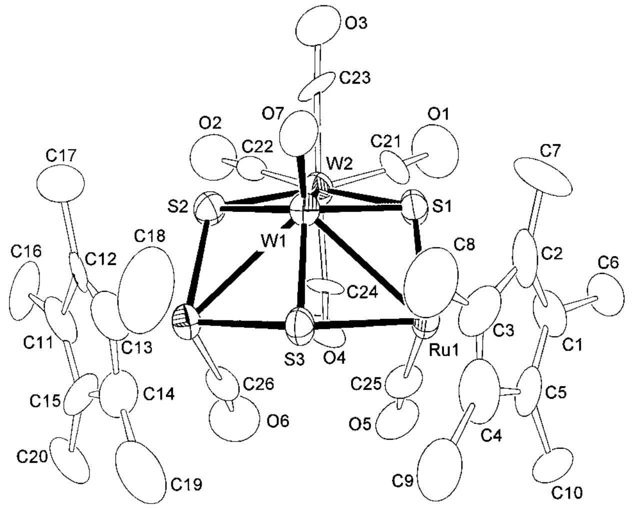

Figure 4. ORTEP drawing of [{Cp*Ru(CO)}$_2${W(μ_3-S)(μ-S)$_2$(=O)}{W(CO)$_4$}] (**4**) with 50% ellipsoids.

The structure of **4** was also determined by an X-ray diffraction study. As shown in Figure 4, **4** is a Ru$_2$W$_2$S$_3$O tetranuclear cluster and its structure is quite similar to that of **2a** except that the terminal S atom in **2a** is replaced by the oxygen atom. Selected interatomic distances and bond angles are listed in Table 4. All three S ligands adopt a μ_3-coordination mode, two of which bridge one Ru and two W atoms and the other one bridges one W and two Ru atoms. The interatomic distance of W1–O7 (1.73(2) Å) is in the normal range expected for a terminal W=O moiety.[11]

Reaction of [Cp*$_2$Ru$_2$S$_4$] with 1 Equiv of [W(CO)$_3$(NCMe)$_3$]. When the reaction of [Cp*$_2$Ru$_2$S$_4$] with 1 equiv of [W(CO)$_3$(NCMe)$_3$] was performed at 50 °C, the Ru$_2$WS$_4$ trinuclear cluster **5a** was obtained in 18% isolated yield (eq 2). Elemental analysis and mass spectral data established that **5a** has the formula Cp*$_2$Ru$_2$WS$_4$(CO)$_2$ and corresponds to the geometric isomer of **3a**. The trinuclear clusters **3a** and **5a** were easily obtained by the reaction of (NH$_4$)$_2$[WS$_4$] with 2 equiv of [Cp*Ru(CO)$_2$Cl] in 45% and 5% yields, respectively (eq 3). Rauchfuss et al. reported a reaction similar to eq 3,

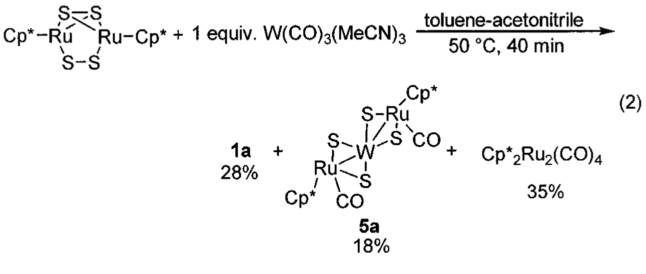

$$(NH_4)_2[WS_4] + 2Cp^*Ru(CO)_2Cl \xrightarrow[\text{reflux, 9 h}]{\text{MeCN}} \underset{45\%}{\mathbf{3a}} + \underset{5\%}{\mathbf{5a}} \quad (3)$$

where [{CpRu(PPh$_3$)}$_2$(WS$_4$)] was obtained by the reaction of (Ph$_4$P)$_2$[WS$_4$] with 2 equiv of [CpRu(PPh$_3$)$_2$Cl].[9a]

---

(10) Sasvári, K. *Acta Crystallogr.* **1963**, *16*, 719.

(11) (a) Müller, A.; Bögge, H.; Hwang, T. K. *Inorg. Chim. Acta* **1980**, *39*, 71. (b) Huang, Q.; Wu, X.; Wang, Q.; Sheng, T.; Lu, J. *Inorg. Chem.* **1996**, *35*, 893. (c) Ogo, S.; Suzuki, T.; Ozawa, Y.; Isobe, K. *Inorg. Chem.* **1996**, *35*, 6093.

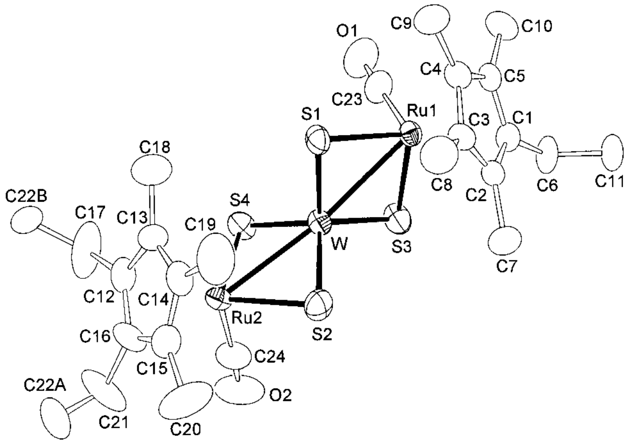

Figure 5. ORTEP drawing of [{(C_5Me_4Et)Ru(CO)}$_2${W(μ-S)$_4$}] (**5b**) with 50% ellipsoids. C22A and C22B represent the β-carbon atom of a disordered ethyl group.

Table 4. Selected Interatomic Distances (Å) and Bond Angles (deg) for [{Cp*Ru(CO)}$_2${W(μ_3-S)$_3$(=O)}{W(CO)$_4$}]·2CH$_2$Cl$_2$ (4·2CH$_2$Cl$_2$)

W1−W2	3.008(2)	W2−S2	2.560(7)
W1−Ru1	2.898(3)	Ru1−S1	2.403(7)
W1−Ru2	2.908(2)	Ru1−S3	2.376(7)
W1−S1	2.289(7)	Ru2−S2	2.414(7)
W1−S2	2.278(7)	Ru2−S3	2.385(7)
W1−S3	2.278(7)	O4···O5	3.10(3)
W1−O7	1.73(2)	O4···O6	3.07(3)
W2−S1	2.572(7)	O5···O6	3.09(3)
W2−W1−Ru1	96.06(6)	S3−W1−O7	110.6(8)
W2−W1−Ru2	95.81(6)	S1−W2−S2	94.8(2)
Ru1−W1−Ru2	94.50(7)	S2−W2−C21	175.4(9)
S1−W1−S2	111.6(3)	S1−W2−C22	175.9(8)
S1−W1−S3	106.2(2)	S1−W2−C23	88.5(9)
S1−W1−O7	110.7(7)	S2−W2−C23	89.3(9)
S2−W1−S3	106.5(2)	C23−W2−C24	171(1)
S2−W1−O7	111.1(7)		

Table 5. Selected Interatomic Distances (Å) and Bond Angles (deg) for [{(C_5Me_4Et)Ru(CO)}$_2${W(μ-S)$_4$}] (5b)

W−Ru	12.891(2)	W−Ru2	2.899(2)
W−S1	2.219(3)	W−S2	2.214(3)
W−S3	2.220(3)	W−S4	2.214(3)
Ru1−S1	2.385(3)	Ru1−S3	2.400(3)
Ru2−S2	2.397(3)	Ru2−S4	2.400(3)
Ru1−W−Ru2	165.51(3)	S2−W−S3	111.2(1)
S1−W−S2	110.9(1)	S2−W−S4	105.9(1)
S1−W−S3	107.6(1)	S3−W−S4	112.0(1)
S1−W−S4	109.2(1)		

The elemental analysis and mass spectral data established the formula of **5a**. In the ^{1}H NMR spectrum of **5a**, a signal assignable to two Cp* ligands was observed as a singlet at 1.68 ppm, indicating the equivalence of two Cp* ligands. The IR spectrum of **5a** shows a CO stretching absorption band in the terminal CO region. The C_5Me_4Et derivatives of **3a** and **5a**, **3b** and **5b**, were also synthesized by the reaction of $(NH_4)_2[WS_4]$ with [(C_5Me_4Et)Ru(CO)$_2$Cl].

The structure of **5b** was unequivocally determined by the X-ray crystal structure analysis. An ORTEP drawing of **5b** is shown in Figure 5. Selected interatomic distances and bond angles are listed in Table 5. The [WS$_4$]$^{2-}$ fragment adopts a slightly distorted tetrahedral geometry with S−W−S angles of 105.9(1)−112.0(1)°. Each of four S atoms is bound to one ruthenium and one tungsten atom in a μ_2-fashion, as observed for [{CpRu(CNMe)}$_2${W(μ-S)$_4$}].[9a] Thus, cluster **1** can be considered as the cluster **5** capped with a W(CO)$_4$ in which the tetrathiotungstate ligand in **5** is coordinated in an η^3-fashion to the tungsten atom by two sulfur and one tungsten atom. The averages of the W−S (2.22 Å) and Ru−S (2.40 Å) distances are also similar to those in [{CpRu(CNMe)}$_2${W(μ-S)$_4$}] (2.21 and 2.39 Å, respectively).[9a] They reflect the unsaturated bonding character of W−S in the tetrathiotungstate moieties.

Reactions of Trinuclear Clusters 3 and 5 with [W(CO)$_3$(NCMe)$_3$]. In the reaction shown in eq 1, trinuclear clusters **3** and **5** are thought to be possible intermediates to give tetranuclear clusters **1** and **2**. To examine this possibility, the reactions of **3a** and **5a** with [W(CO)$_3$(NCMe)$_3$] were performed. When a solution of the trinuclear cluster **3a** was heated, followed by treatment with CO, **3a** was converted to **2a** with small amounts of **1a** and **4** (eq 4). On the other hand, thermal reaction of **5a**, followed by treatment with CO, led to the exclusive formation of **1a** in 87% isolated yield (eq 5). Before treatment with CO, TLC analysis showed a brown spot which is tentatively assigned to the MeCN-substituted cluster [{Cp*Ru(CO)}$_2${W(μ_3-S)$_2$(μ-S)$_2$)}{W(CO)$_3$(NCMe)}] (**6**). Although isolation of **6** was unsuccessful due to its instability, the ^{t}BuNC derivative [{Cp*Ru(CO)}$_2${W(μ_3-S)$_2$(μ-S)$_2$)}{W(CO)$_3$(CN^{t}Bu)}] (**7**) was unequivocally characterized. Treatment of the reaction mixture, resulting from the reaction of **5a** and [W(CO)$_3$(NCMe)$_3$], with ^{t}BuNC led to the formation of **1a** and **7** (eq 6). At this stage, the brown spot of **6** disappeared from TLC analysis. These results are consistent with the formation of **6** in the thermal reaction of **5a** and [W(CO)$_3$(NCMe)$_3$].

$$\mathbf{3a} + \mathrm{W(CO)_3(MeCN)_3} \xrightarrow[\substack{\text{1) 50 °C, 30 min} \\ \text{2) +CO, r.t., 10 min}}]{\text{toluene-acetonitrile}} \underset{9\%}{\mathbf{1a}} + \underset{47\%}{\mathbf{2a}} + \underset{12\%}{\mathbf{4}} \quad (4)$$

$$\mathbf{5a} + \mathrm{W(CO)_3(MeCN)_3} \xrightarrow[\substack{\text{1) 50 °C, 30 min} \\ \text{2) +CO, r.t., 10 min}}]{\text{toluene-acetonitrile}} \underset{87\%}{\mathbf{1a}} \quad (5)$$

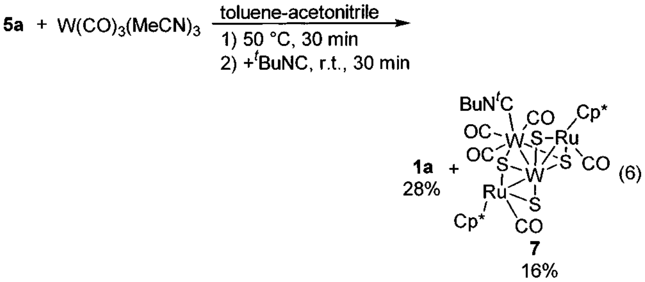

An ORTEP drawing of **7** is shown in Figure 6, and the selected interatomic distances and bond angles are listed in Table 6. The structure of **7** is similar to that of **1a**, except that a carbonyl ligand is replaced by a ^{t}BuNC ligand. The W2 atom with three CO, two S, and one ^{t}BuNC ligand adopts a distorted-octahedral geometry, and three CO ligands occupy the *fac* positions. The bond angles of W2−C26−N and C26−N−C27 are 167(2) and 172(2)°, respectively. They reflect the steric

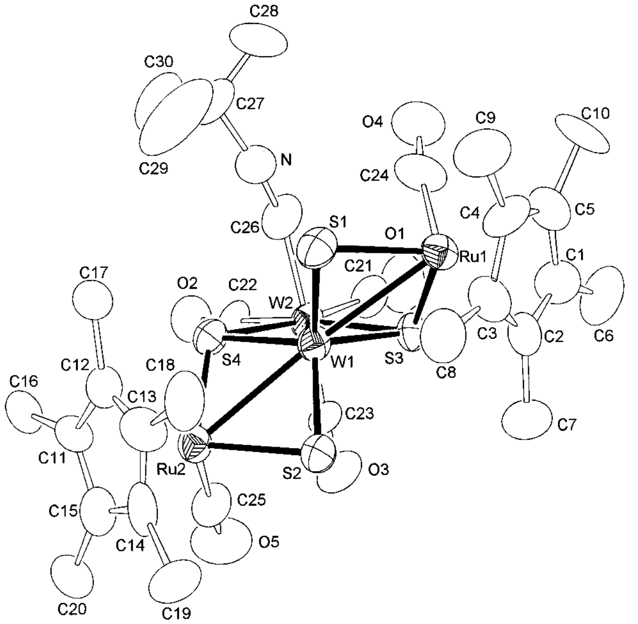

Figure 6. ORTEP drawing of [{Cp*Ru(CO)}$_2${W(μ_3-S)$_2$(μ-S)$_2$}{W(CO)$_3$(CN^{t}Bu)}] (**7**) with 50% ellipsoids.

Table 6. Selected Interatomic Distances (Å) and Bond Angles (deg) for [{Cp*Ru(CO)}$_2${W(μ_3-S)$_2$(μ-S)$_2$}{W(CO)$_3$(CN^{t}Bu)}] (7)

W1–W2	2.876(1)	W2–S4	2.537(5)
W1–Ru1	2.892(2)	Ru1–S1	2.416(6)
W1–Ru2	2.884(2)	Ru1–S3	2.389(5)
W1–S1	2.234(6)	Ru2–S2	2.401(6)
W1–S2	2.207(5)	Ru2–S4	2.380(5)
W1–S3	2.274(5)	O3···O5	3.04(3)
W1–S4	2.270(5)	O4···N	3.37(3)
W2–S3	2.545(5)	O4···C26	3.40(3)
		O4···C28	3.60(4)
W2–W1–Ru1	97.96(4)	S3–W1–S4	115.5(2)
W2–W1–Ru2	97.76(4)	S2–W2–S4	98.2(2)
Ru1–W1–Ru2	164.22(5)		
S1–W1–S2	113.6(2)	Ru1–C24–O4	170(2)
S1–W1–S3	106.1(2)	Ru1–C25–O5	178(2)
S1–W1–S4	107.2(2)	W2–C26–N	167(2)
S2–W1–S3	107.9(2)	C26–N–C27	172(2)
S2–W1–S4	106.8(2)		

repulsion between a ^{t}BuNC and a CO ligand (C28···O4 = 3.60(4) Å).

Isomerization Reactions between 1a and 2a. Under the same conditions as those in eq 1 (50 °C, 40 min), isomerization reactions between **1a** and **2a** and between **3a** and **5a** were not observed at all. Thermal reactions of **2a** and **3a** at 80 °C resulted in isomerization to give **1a** (eq 7) and **5a** (eq 8), respectively. The thermal

$$\mathbf{2a} \xrightarrow[80\ ^\circ\mathrm{C},\ 2\ \mathrm{h}]{C_6D_6} \underset{ca.\ 90\%}{\mathbf{1a}} \qquad (7)$$

$$\mathbf{3a} \xrightarrow[80\ ^\circ\mathrm{C},\ 2\ \mathrm{days}]{C_6D_6\text{-}CD_3CN} \underset{ca.\ 40\%}{\mathbf{5a}} \qquad (8)$$

instability of the isomers **2a** and **3a** with a terminal S ligand compared with **1a** and **5a** may come from the steric repulsion between carbonyl ligands on one tungsten and two ruthenium metals as observed in the crystal structure of **2a** and **3a**. Photolysis of a benzene-d_6 solution of **1a** in a Pyrex tube for 1 h led to disappearance of **1a** to give **2a** in ca. 50% yield (eq 9). On the other hand, irradiation of **5a** in benzene-d_6 gave several unidentified products, and formation of its geometric isomer **3a** was not confirmed (eq 10).

Scheme 1

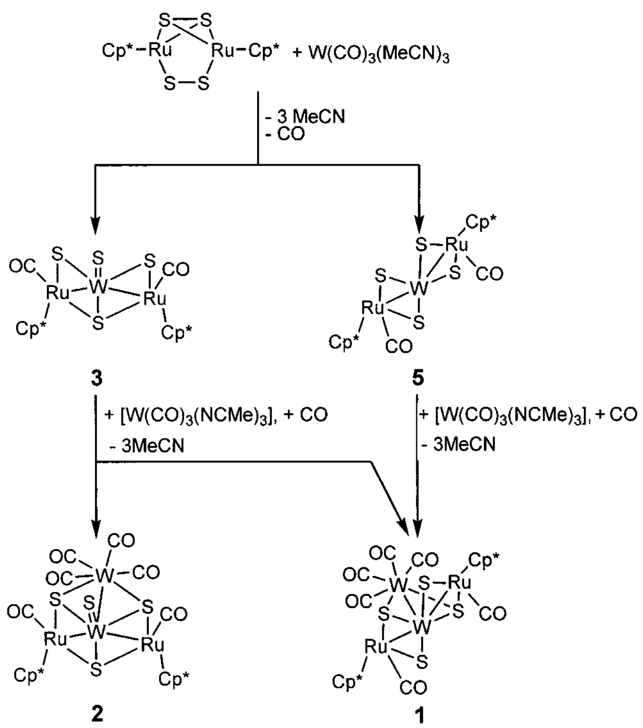

$$\mathbf{1a} \xrightarrow[\mathrm{r.t.,\ 1\ h}]{h\nu,\ C_6D_6} \underset{ca.\ 50\%}{\mathbf{2a}} \qquad (9)$$

$$\mathbf{5a} \xrightarrow[\mathrm{r.t.,\ 12\ h}]{h\nu,\ C_6D_6} \text{unidentified products} \qquad (10)$$

Cross-Reaction with [W(CO)$_3$(NCMe)$_3$] using [Cp*$_2$Ru$_2$S$_4$] and [(C$_5$Me$_4$Et)$_2$Ru$_2$S$_4$]. The cross-reaction of a 1:1 molar mixture of [Cp*$_2$Ru$_2$S$_4$] and [(C$_5$Me$_4$Et)$_2$Ru$_2$S$_4$] with [W(CO)$_3$(NCMe)$_3$] gave **1a**, **2a**, **1b**, and **2b** in 40, 10, 47, and 14% yields, respectively (eq 11). Small amounts of **5a** and **5b** were also formed.

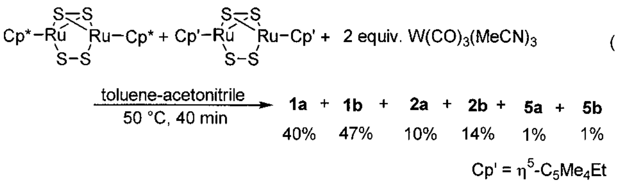

(11)

No crossover products such as [{Cp*Ru(CO)}{(C$_5$Me$_4$Et)-Ru(CO)}{W(μ_3-S)$_2$(μ-S)$_2$)}{W(CO)$_4$}] and [{Cp*Ru(CO)}{(C$_5$Me$_4$Et)Ru(CO)}{W(μ_3-S)$_3$(=S)}{W(CO)$_4$}] were detected, which indicates that clusters **1** and **2** are formed without the rupture of ruthenium dimer.

Formation Mechanism of 1 and 2. A plausible reaction pathway for the formation of **1** and **2** is illustrated in Scheme 1. The reaction of [Cp*$_2$Ru$_2$S$_4$] with [W(CO)$_3$(NCMe)$_3$] gives two kinds of trinuclear clusters, **3** and **5**, without rupture of the ruthenium dimer via liberation of one CO and three MeCN ligands. In the paths, reorganization of CO and S ligands took place between one W and two Ru atoms. Upon subsequent reactions of **3** and **5** with [W(CO)$_3$(NCMe)$_3$] and CO, cluster **3** is converted to **2** with a small amount of **1**, whereas **5** is converted to **1** exclusively.

Table 7. Cyclic Voltammetric Data for the Clusters[a]

compd	potentials[b]		
	$E_{p,a}$	$E_{p,c}$	$E_{1/2}$
1a	+607		
1a[c]	+643	+524	+584
2a	+382	+308	+345
3a	+653		
4	+337	+252	+295
5a	+713		
7	+251	+163	+207

[a] Each cluster exhibits one-electron oxidation wave. [b] Potentials are given in mV vs Ag/0.01 M $AgNO_3$−MeCN. The scan rate is 50 mV s^{-1}, unless otherwise stated. [c] Scan rate: 500 mV s^{-1}.

The tetrathiometalates have been widely studied as ligands for transition metals, and their reactions have been carried out with many transition-metal halides to give various homo- and heterometallic sulfide clusters.[12] To our knowledge, only two examples have been known for the synthesis of clusters containing tetrathiometalates $[MS_4]^{2-}$ (M = Mo, W), which were not derived from salt-elimination reactions of tetrathiometalates with metal halide.[13] Huang and Kanatzidis reported that $[M(CO)_6]$ (M = Mo, W) reacted with Na_2S_2 in the presence of Ph_4PCl to give the tetrathiometalate clusters $(Ph_4P)_2[(CO)_4M(MS_4)]$.[13a] Boorman et al. described the synthesis of the tetrathiomolybdate cluster $[(Cp_2Nb)_2MoS_4]$ by the reaction of $[Cp_2NbH_3]$ and $[Mo(S^tBu)_4]$ in benzene via evolution of isobutane.[13b] In connection with the formation of tetrathiometalate anion, Tatsumi et al. reported that the thermal decomposition of $(Ph_4P)[Cp^*Mo(SCH_2CH_2S)_2]$ at 140 °C gave $(Ph_4P)_2[MoS_4]$.[14]

Electrochemistry. Cyclic voltammetric data for **1a**, **2a**, **3a**, **4**, **5a**, and **7** are summarized in Table 7. Tetranuclear clusters **1a**, **2a**, **4**, and **7** undergo reversible or quasi-reversible one-electron oxidation, whereas trinuclear clusters **3a** and **5a** undergo irreversible one-electron oxidation. The potentials are affected by both nuclearity and coordination mode of the $[WS_4]^{2-}$ ligand. Tetranuclear clusters exhibit relatively low one-electron-oxidation potential compared to trinuclear clusters. The $[WS_3O]^{2-}$ cluster **4** exhibits a lower one-electron-oxidation potential than the corresponding $[WS_4]^{2-}$ cluster **2** by 50 mV. In comparison with **1a** ($E_{1/2}$ = +584 mV), the ^{t}BuNC derivative **7** ($E_{1/2}$ = +207 mV) has a considerably lower oxidation potential, which reflects the strong σ-donor ability of the ^{t}BuNC ligand.

Summary

We have investigated heterometallic cluster construction by the reactions of $[Cp^*_2Ru_2S_4]$ with $[W(CO)_3(NCMe)_3]$. The reactions afforded two isomeric pairs of tetrathiotungstate trinuclear and tetranuclear clusters, $[\{Cp^*Ru(CO)\}_2(WS_4)]$ and $[\{Cp^*Ru(CO)\}_2(WS_4)\{W(CO)_4\}]$. The trinuclear clusters were converted to the tetranuclear clusters by the reaction with $[W(CO)_3(NCMe)_3]$, followed by treatment with CO. Thus, the former clusters are considered to be intermediates to give the tetranuclear clusters.

Experimental Section

General Information and Materials. Infrared spectra were recorded on a Horiba FT-200 spectrometer. ^{1}H and ^{13}C NMR spectra were recorded on a Bruker ARX-300 instrument. Mass spectra were recorded on a JEOL-HX110 instrument operating in the fast atom bombardment (FAB) mode. All reactions were performed under a nitrogen atmosphere using deoxygenated solvents dried with appropriate reagents. $[W(CO)_6]$ was used as purchased. The complexes $[Cp^*_2Ru_2S_4]$,[15] $[(C_5Me_4Et)_2Ru_2S_4]$,[15] $[W(CO)_3(NCMe)_3]$,[16] $(NH_4)_2[WS_4]$,[17] $[Cp^*Ru(CO)_2Cl]$,[18] and $[(C_5Me_4Et)Ru(CO)_2Cl]$[18] were prepared by published procedures. Photochemical reactions were performed with an Ushio UM-452 medium-pressure mercury lamp. Electrochemical measurements were carried out on a BAS-100 electrochemical analyzer in dichloromethane solutions containing 0.1 M Bu_4NBF_4 as a supporting electrolyte and 1 mM compound. Potentials are reported as mV versus Ag/0.01 M $AgNO_3$−MeCN. Cyclic voltammetry data were recorded at 50 mV s^{-1} scan rate at room temperature, unless noted otherwise. Under these conditions, the ferrocene/ferrocenium couple is at +201 mV versus Ag/0.01 M $AgNO_3$−MeCN.

Reaction of $[Cp^*_2Ru_2S_4]$ with 2 Equiv of $[W(CO)_3(NCMe)_3]$. To an acetonitrile solution of $[W(CO)_3(NCMe)_3]$, which was prepared by refluxing an acetonitrile (5 mL) solution of $[W(CO)_6]$ (189 mg, 0.536 mmol), was added a toluene (15 mL) solution of $[Cp^*_2Ru_2S_4]$ (161 mg, 0.268 mmol). The solution was heated at 50 °C for 40 min. Volatiles were removed under reduced pressure, and the residue was dissolved in 10 mL of a toluene/hexane (1/1) mixture. Dark brown insoluble material (**A**) was filtered off and collected. The filtrate was charged on a silica gel flash column. Elution with a toluene/hexane (1/1) mixture and then with toluene afforded a reddish brown band and an orange band. The eluates were concentrated to dryness to give $[\{Cp^*Ru(CO)\}_2\{W(\mu_3\text{-}S)_2(\mu\text{-}S)_2\}\{W(CO)_4\}]$ (**1a**; 177 mg, 58%) and $[\{Cp^*Ru(CO)\}_2\{W(\mu_3\text{-}S)(\mu\text{-}S)_2({=}S)\}]$ (**3a**; 19 mg, 8%), respectively. The dark brown solid **A** was dissolved in dichloromethane and subjected to silica gel flash column chromatography. The reddish brown fraction of $[\{Cp^*Ru(CO)\}_2\{W(\mu_3\text{-}S)_3({=}S)\}\{W(CO)_4\}]$ (**2a**; 35 mg, 11%) and the dark green fraction of $[\{Cp^*Ru(CO)\}_2\{W(\mu_3\text{-}S)_3({=}O)\}\{W(CO)_4\}]$ (**4**; 12 mg, 4%) were collected in this order with dichloromethane as an eluent. After removal of volatiles, analytically pure samples of the compounds were obtained by recrystallization from toluene−hexane at −30 °C for **2a** and from dichloromethane−hexane at −30 °C for **1a**, **3a**, and **4**. Data for **1a**: MS (FAB, ^{102}Ru, ^{184}W) m/z 1138 (M^+); IR (KBr) 2031, 1975, 1959, 1921, 1848 (ν_{CO}) cm^{-1}; ^{1}H NMR (C_6D_6) δ 1.68 (s, 30 H, Cp*); ^{13}C NMR (C_6D_6) δ 207.8, 204.3, 200.5 (CO), 100.5 (C_5Me_5), 10.2 (C_5Me_5); UV−visible (toluene) λ_{max}/nm (ϵ/cm^{-1} M^{-1}) 314 (1.7×10^4), 349 (1.5×10^4), 408 (1.2×10^4), 480 (sh),

---

[12] See for examples: (a) Jeannin, Y.; Sécheresse, F.; Bernès, S.; Robert, F. *Inorg. Chim. Acta* **1992**, *198-200*, 493. (b) Königer-Ahlborn, E.; Müller, A. *Angew. Chem., Int. Ed. Engl.* **1976**, *15*, 680. (c) Yu, H.; Zhang, W.; Wu, X.; Sheng, T.; Wang, Q.; Lin, P. *Angew. Chem., Int. Ed.* **1998**, *37*, 2520. (d) Howard, K. E.; Rauchfuss, T. B.; Wilson, S. R. *Inorg. Chem.* **1988**, *27*, 3561. (e) Bencini, A.; Cecconi, F.; Ghilardi, C. A.; Midollini, S.; Nuzzi, F.; Orlandini, A. *Inorg. Chem.* **1992**, *31*, 5339. (f) Shapley, P. A.; Gebeyehu, Z.; Zhang, N.; Wilson, S. R. *Inorg. Chem.* **1993**, *32*, 5646. (g) Sánchez, G.; Momblona, F.; García, G.; López, G.; Pinilla, E.; Monge, A. *J. Chem. Soc., Dalton Trans.* **1994**, 2271. (h) Evans, W. J.; Ansari, M. A.; Ziller, J. W. *Organometallics* **1995**, *14*, 3. (i) Canales, F.; Gimeno, M. C.; Jones, P. G.; Laguna, A. *J. Chem. Soc., Dalton Trans.* **1997**, 439.

[13] (a) Huang, S.-P.; Kanatzidis, M. G. *Inorg. Chim. Acta* **1995**, *230*, 9. (b) Boorman, P. M.; Fait, J. F.; Freeman, G. K. W. *Polydedron* **1989**, *8*, 1762.

[14] Kawaguchi, H.; Yamada, K.; Lang, J.-P.; Tatsumi, K. *J. Am. Chem. Soc.* **1997**, *119*, 10346.

[15] Rauchfuss, T. B.; Rodgers, D. P. S.; Wilson, S. R. *J. Am. Chem. Soc.* **1986**, *108*, 3114.

[16] Tate, D. P.; Knipple, W. R.; Augl, J. M. *Inorg. Chem.* **1962**, *1*, 433.

[17] Pan, W.-H.; Leonowicz, M. E.; Stiefel, E. I. *Inorg. Chem.* **1983**, *22*, 672.

[18] Oshima, N.; Suzuki, H.; Moro-oka, Y. *Chem. Lett.* **1984**, 1161.

535 (sh). Anal. Calcd for $C_{26}H_{30}O_6Ru_2S_4W_2$: C, 27.48; H, 2.66. Found: C, 27.83; H, 2.74. Data for **2a**: MS (FAB, ^{102}Ru, ^{184}W) *m/z* 1138 (M$^+$); IR (KBr) 2019, 1975, 1905 (sh), 1882 (ν_{CO}) cm^{-1}; ^{1}H NMR (C_6D_6) δ 1.59 (s, 30 H, Cp*); ^{13}C NMR (CD_2Cl_2) δ 209.7, 208.1, 205.3, 196.2 (CO), 100.4 (*C*$_5$Me$_5$), 10.3 (C$_5$*Me*$_5$); UV−visible (toluene) λ_{max}/nm (ϵ/cm^{-1} M^{-1}) 325 (2.4×10^4), 429 (1.1×10^4), 510 (8.2×10^3), 682 (2.3×10^3). Anal. Calcd for $C_{26}H_{30}O_6Ru_2S_4W_2$: C, 27.48; H, 2.66. Found: C, 27.71; H, 2.95. Data for **3a**: MS (FAB, ^{102}Ru, ^{184}W) *m/z* 842 (M$^+$); IR (KBr) 1969 (ν_{CO}) cm^{-1}; ^{1}H NMR (C_6D_6) δ 1.64 (s, 30 H, Cp*); ^{13}C NMR (C_6D_6) δ 204.8 (CO), 99.6 (*C*$_5$Me$_5$), 10.1 (C$_5$*Me*$_5$). Anal. Calcd for $C_{22}H_{30}O_2Ru_2S_4W$: C, 31.14; H, 3.60. Found: C, 31.66; H, 3.70. Data for **4**: MS (FAB, ^{102}Ru, ^{184}W) *m/z* 1122 (M$^+$); IR (KBr) 2021, 1979, 1892, 1880 (ν_{CO}), 943 (ν_{WO}) cm^{-1}; ^{1}H NMR (C_6D_6) δ 1.53 (s, 30 H, Cp*); ^{13}C NMR (C_6D_6) δ 209.6, 207.6, 204.9, 195.7 (CO), 100.2 (*C*$_5$Me$_5$), 10.2 (C$_5$*Me*$_5$). Anal. Calcd for $C_{28}H_{34}Cl_4O_7Ru_2S_3W_2$: C, 26.06; H, 2.66. Found: C, 26.83; H, 2.98.

Reaction of $[(C_5Me_4Et)_2Ru_2S_4]$ with 2 Equiv of $[W(CO)_3(NCMe)_3]$. To an acetonitrile solution of $[W(CO)_3(NCMe)_3]$, which was prepared by refluxing an acetonitrile (5 mL) solution of $[W(CO)_6]$ (101 mg, 0.287 mmol), was added a toluene (15 mL) solution of $[(C_5Me_4Et)_2Ru_2S_4]$ (84 mg, 0.134 mmol). Workup of the resulting solution similar to that of the Cp* system afforded $[\{(C_5Me_4Et)Ru(CO)\}_2\{W(\mu_3\text{-}S)_2(\mu\text{-}S)_2\}\{W(CO)_4\}]$ (**1b**; 61 mg, 39%), $[\{(C_5Me_4Et)Ru(CO)\}_2\{W(\mu_3\text{-}S)_3({=}S)\}\{W(CO)_4\}]$ (**2b**; 18 mg, 12%), and $[\{(C_5Me_4Et)Ru(CO)\}_2\{W(\mu_3\text{-}S)(\mu\text{-}S)_2({=}S)\}]$ (**3b**; 9 mg, 8%). Data for **1b**: MS (FAB, ^{102}Ru, ^{184}W) *m/z* 1166 (M$^+$); IR (KBr) 2031, 1961, 1913, 1892 cm^{-1} (ν_{CO});^{1}H NMR (300 MHz, C_6D_6) δ 2.34−2.25 (m, 4H, C*H*$_2$CH$_3$), 1.75 (s, 6H, Me), 1.73 (s, 6H, Me), 1.68 (s, 6H, Me), 1.67 (s, 6H, Me), 0.82 (t, $J = 8$ Hz, 6H, CH$_2$C*H*$_3$); ^{13}C NMR (75 MHz, C_6D_6) δ 207.7, 204.1, 200.5 (CO), 103.2, 101.6, 101.1, 101.0, 100.4 (*C*$_5$Me$_4$Et), 19.3 (CH$_2$), 15.0, 10.03, 10.02, 10.01, 9.9 (CH$_3$). Anal. Calcd for $C_{28}H_{34}O_6Ru_2S_4W_2$: C, 28.88; H, 2.94. Found: C, 29.17; H, 2.98. Data for **2b**: MS (FAB, ^{102}Ru, ^{184}W) *m/z* 1166 (M$^+$); IR (KBr) 2021, 1973, 1927 (sh), 1913 (sh), 1892 cm^{-1} (ν_{CO}); ^{1}H NMR (300 MHz, C_6D_6) δ 2.23−2.18 (m, 4H, C*H*$_2$CH$_3$), 1.66 (s, 6H, Me), 1.64 (s, 6H, Me), 1.60 (s, 6H, Me), 1.59 (s, 6H, Me), 0.78 (t, $J = 8$ Hz, 6H, CH$_2$C*H*$_3$); ^{13}C NMR (75 MHz, C_6D_6) δ 210.1, 207.9, 204.9, 195.9 (CO), 102.0, 100.4, 100.1, 100.0, 99.4 (*C*$_5$Me$_4$Et), 18.9 (CH$_2$), 14.7, 9.63, 9.57, 9.50 (CH$_3$). Anal. Calcd for $C_{28}H_{34}O_6Ru_2S_4W_2$: C, 28.88; H, 2.94. Found: C, 29.44; H, 3.00. Data for **3b**: MS (FAB, ^{102}Ru, ^{184}W) *m/z* 870 (M$^+$); IR (KBr) 1971 cm^{-1} (ν_{CO}); ^{1}H NMR (300 MHz, C_6D_6) δ 2.29 (q, $J = 8$ Hz, 4H, C*H*$_2$CH$_3$), 1.74 (s, 6H, Me), 1.69 (s, 6H, Me), 1.65 (s, 6H, Me), 1.60 (s, 6H, Me), 0.80 (t, $J = 8$ Hz, 6H, CH$_2$C*H*$_3$);^{13}C NMR (75 MHz, C_6D_6) δ 204.6 (CO), 102.2, 100.54, 100.47, 99.9, 99.6 (*C*$_5$Me$_4$Et), 19.2 (CH$_2$), 14.9, 9.89, 9.87, 9.85, 9.79 (CH$_3$). Anal. Calcd for $C_{24}H_{34}O_2Ru_2S_4W$: C, 33.18; H, 3.94. Found: C, 33.47; H, 3.85.

Reaction of $[Cp^*{}_2Ru_2S_4]$ with 1 Equiv of $[W(CO)_3(NCMe)_3]$. To an acetonitrile solution of $[W(CO)_3(NCMe)_3]$, which was prepared by refluxing an acetonitrile (3 mL) solution of $[W(CO)_6]$ (98 mg, 0.28 mmol), was added a toluene (9 mL) solution of $[Cp^*{}_2Ru_2S_4]$ (166 mg, 0.277 mmol). The solution was heated at 50 °C for 50 min. Volatiles were removed under reduced pressure, and the residue was charged on a silica gel flash column. Elution was carried out with a toluene/hexane (1/1) mixture, and eluents were separated in five fractions in the following order: $[Cp^*{}_2Ru_2(CO)_4]$ (13 mg, 22 μmol); 10:10:1 molar mixture (28 mg) of $[Cp^*{}_2Ru_2(CO)_4]$ (16 μmol), **1a** (16 μmol), and $[\{Cp^*Ru(CO)\}_2\{W(\mu\text{-}S)_4\}]$ (**5a**) (2 μmol); **5a** (11 mg, 13 μmol); 1:9 molar mixture (30 mg) of **5a** (43 μmol) and $[Cp^*{}_2Ru_2S_4]$ (5 μmol); $[Cp^*{}_2Ru_2S_4]$ (75 mg, 124 μmol). The molar ratio of each compound was determined on the basis of the intensity of the ^{1}H NMR signals. Total yield: **1a**, 28%; **5a**, 18%; recovery of $[Cp^*{}_2Ru_2S_4]$, 60%; $[Cp^*{}_2Ru_2(CO)_4]$, 35%. **5a** was recrystallized from ether at −30 °C to give analytically pure fine needles. Data for **5a**: MS (FAB, ^{102}Ru, ^{184}W) *m/z* 842 (M$^+$); IR (KBr) 1944 (ν_{CO}) cm^{-1}; ^{1}H NMR (300 MHz, C_6D_6) δ 1.68 (s, 30 H, Cp*); ^{13}C NMR (75.5 MHz, C_6D_6) δ 202.8 (CO), 100.5 (*C*$_5$Me$_5$), 10.4 (C$_5$*Me*$_5$). Anal. Calcd for $C_{22}H_{30}O_2Ru_2S_4W$: C, 31.43; H, 3.60; S, 15.26. Found: C, 32.06; H, 3.73; S, 15.12.

Synthesis of 3a and 5a by the Reaction of $(NH_4)_2[WS_4]$ with $[Cp^*Ru(CO)_2Cl]$. An acetonitrile solution (50 mL) of $[Cp^*Ru(CO)_2Cl]$ (3.58 g, 10.9 mmol) and $(NH_4)_2[WS_4]$ (1.77 g, 5.09 mmol) was refluxed for 9 h. After the reaction mixture was cooled, volatiles were removed under reduced pressure and the residue was extracted with toluene. The toluene extract was subjected to silica gel flash column chromatography and two separate orange bands were collected with toluene as an eluent. Concentration of the fractions afforded **3a** (223 mg, 5%) and **5a** (1.92 g, 45%), respectively.

Synthesis of 3b and 5b by the Reaction of $(NH_4)_2[WS_4]$ with $[(C_5Me_4Et)Ru(CO)_2Cl]$. An acetonitrile solution (50 mL) of $[(C_5Me_4Et)Ru(CO)_2Cl]$ (3.86 g, 11.3 mmol) and $(NH_4)_2[WS_4]$ (2.00 g, 5.75 mmol) was refluxed for 8 h. Workup of the resulting solution in a manner similar to that for the Cp* system gave **3b** (518 mg, 11%) and $[\{(C_5Me_4Et)Ru(CO)\}_2\{W(\mu\text{-}S)_4\}]$ (**5b**; 1.31 g, 27%). Data for **5b**: MS (FAB, ^{102}Ru, ^{184}W) *m/z* 842 (M$^+$ − CO); IR (KBr) 1942 cm^{-1} (ν_{CO}); ^{1}H NMR (300 MHz, C_6D_6) δ 2.32 (q, $J = 8$ Hz, 4H, C*H*$_2$CH$_3$), 1.759 (s, 6H, Me), 1.755 (s, 6H, Me), 1.658 (s, 6H, Me), 1.652 (s, 6H, Me), 0.81 (t, $J = 8$ Hz, 6H, CH$_2$C*H*$_3$); ^{13}C NMR (75 MHz, C_6D_6) δ 202.6 (CO), 103.4, 101.40, 101.39, 100.7, 100.6 (*C*$_5$Me$_4$Et), 19.6 (CH$_2$), 15.1 (Me × 2), 10.20 (Me × 6), 10.18 (Me × 2). Anal. Calcd for $C_{24}H_{34}O_2Ru_2S_4W$: C, 33.18; H, 3.94. Found: C, 33.40; H, 3.87.

Reaction of 3a with $[W(CO)_3(NCMe)_3]$ and CO. To an acetonitrile solution of $[W(CO)_3(NCMe)_3]$, which was prepared by refluxing an acetonitrile (5 mL) solution of $[W(CO)_6]$ (106 mg, 0.302 mmol), was added a toluene (15 mL) solution of **3a** (152 mg, 0.181 mmol). The reaction mixture was heated at 50 °C for 30 min. After the solution was cooled to room temperature, CO gas was bubbled through the solution for 10 min. Volatiles were removed under reduced pressure and the residue was subjected to silica gel flash column chromatography. Elution with a toluene/hexane (1/1) mixture afforded **1a** (19 mg, 9%), **2a** (96 mg, 47%), and unreacted **3a** (14 mg, 9%) in this order. Subsequently, elution with dichloromethane afforded **4** (25 mg, 12%).

Reaction of 5a with $[W(CO)_3(NCMe)_3]$ and CO. To an acetonitrile solution of $[W(CO)_3(NCMe)_3]]$, which was prepared by refluxing an acetonitrile (5 mL) solution of $W(CO)_6$ (112 mg, 0.319 mmol), was added a toluene (15 mL) solution of **5a** (189 mg, 0.225 mmol). The reaction mixture was heated at 50 °C for 30 min. At this stage, TLC (toluene) showed spots assignable to **1a**, unreacted **5a**, and $[\{Cp^*Ru(CO)\}_2\{W(\mu_3\text{-}S)_2(\mu\text{-}S)_2\}\{W(CO)_3(NCMe)\}]$ (**6**) ($R_f = 0.2$). After the resulting solution was cooled, CO gas was bubbled through the solution for 10 min. The color of the solution changed from dark brown to reddish brown, and the spot assignable to **6** disappeared from TLC analysis. Volatiles were removed under reduced pressure, and the residue was subjected to silica gel flash column chromatography. Elution with a toluene/hexane (1/1) mixture and concentration of two separate fractions afforded **1a** (222 mg, 87%) and unreacted **5a** (4 mg, 2%) in this order.

Reaction of 6 with ^{t}BuNC. To an acetonitrile solution of $[W(CO)_3(NCMe)_3]$, which was prepared by refluxing an acetonitrile (5 mL) solution of $[W(CO)_6]$ (55 mg, 0.16 mmol), was added a toluene (15 mL) solution of **5a** (128 mg, 0.153 mmol). The reaction mixture was heated at 50 °C for 25 min. At this stage, TLC (toluene) showed spots assignable to **1a**, **5a**, and **6**. After the resulting solution was cooled, ^{t}BuNC (15 mg, 0.18 mmol) was added and the mixture was stirred at room temperature for 30 min. Volatiles were removed under reduced pressure, and the residue was charged on a silica gel flash column. Elution with a toluene/hexane (1/1) mixture and

Table 8. Summary of Crystallographic Parameters

	1a	**2a**·$2CH_2Cl_2$	**3a**	**4**·$2CH_2Cl_2$	**5b**	**7**
formula	$C_{26}H_{30}O_6Ru_2S_4W_2$	$C_{28}H_{34}Cl_4O_6Ru_2S_4W_2$	$C_{22}H_{30}O_2Ru_2S_4W$	$C_{28}H_{34}Cl_4O_7Ru_2S_3W_2$	$C_{24}H_{34}O_2Ru_2S_4W$	$C_{30}H_{39}NO_5Ru_2S_4W_2$
fw	1136.60	1306.47	840.71	1290.40	868.76	1191.72
a, Å	22.41(1)	15.642(8)	8.260(7)	15.564(7)	13.985(8)	10.719(3)
b, Å	13.432(6)	11.132(6)	35.77(2)	11.056(6)	14.701(5)	9.531(4)
c, Å	11.148(3)	23.463(4)	9.695(7)	23.586(8)	15.421(5)	38.28(1)
β, deg	90.07(3)	96.64(2)	106.50(7)	97.92(3)	113.44(3)	97.19(2)
V, Å^3	3355(2)	4058(2)	2746(3)	4019(3)	2908(2)	3880(2)
space group	$P2_1/n$	$P2_1/c$	$P2_1/c$	$P2_1/c$	$P2_1/n$	$P2_1/c$
Z	4	4	4	4	4	4
d_{calcd}, g cm^{-3}	2.249	2.138	2.033	2.132	1.98	2.04
d_{obsd}, g cm^{-3}	2.23	2.1	2.00	2.1	1.96	2.02
cryst size, mm	0.50 × 0.40 × 0.25	0.30 × 0.20 × 0.15	0.50 × 0.50 × 0.15	0.20 × 0.20 × 0.08	0.50 × 0.15 × 0.15	0.25 × 0.20 × 0.20
μ(Mo Kα), cm^{-1}	80.08	68.92	55.90	69.08	52.81	69.30
transmissn factor range	1.00−0.73	1.00−0.80	1.00−0.46	1.00−0.69	1.00−0.44	1.00−0.62
2θ range, deg	3−55	3−55	3−50	3−50	3−55	3−50
scan mode	$\omega-2\theta$	$\omega-2\theta$	ω	$\omega-2\theta$	$\omega-2\theta$	ω
ω-scan width, deg	$1.1 + 0.35 \tan\theta$	$1.0 + 0.35 \tan\theta$	$1.6 + 0.35 \tan\theta$	$1.1 + 0.35 \tan\theta$	$1.0 + 0.35 \tan\theta$	$1.2 + 0.35 \tan\theta$
ω-scan rate, deg min^{-1}	4.0	4.0	4.0	4.0	4.0	4.0
no. of unique data collected	8049	9816	4948	7489	6671	7270
no. of data used with $I > 3\sigma(I)$	4762	3634	2772	2978	4061	3170
no. of params refined	361	415	280	397	308	397
final R	0.045	0.056	0.065	0.058	0.044	0.046
final R_w	0.064	0.075	0.102	0.075	0.063	0.055
final GOF	0.96	1.02	1.27	1.09	0.91	1.09
largest shift/esd in final cycle	0.16	0.49	0.45	0.65	0.02	0.05
max resid electron dens, e Å^{-3}	1.09	2.12	1.97	2.23	0.74	1.08

concentration of three fractions afforded **1a** (48 mg, 28%), brown solid (66 mg) containing **5a**, one more product,[19] and [{Cp*Ru(CO)}$_2${W(μ_3-S)$_2$(μ-S)$_2$}{W(CO)$_3$(CN^{t}Bu)}] (**7**; 29 mg, 16%) in that order. Cluster **7** was recrystallized from a dichloromethane−hexane mixture to give brown crystals. Data for **7**: MS (FAB, ^{102}Ru, ^{184}W) m/z 1193 (M$^+$); IR (KBr) 2121 (ν_{CN}), 1979, 1948, 1934, 1888, 1871 (ν_{CO}) cm^{-1}; ^{1}H NMR (300 MHz, C_6D_6) δ 1.794 (s, 15H, Cp*), 1.789 (s, 15H, Cp*), 0.76 (s, 9H, ^{t}Bu); ^{13}C NMR (75.5 MHz, C_6D_6) δ 214.7, 214.6, 207.2, 206.5, 203.6 (CO), 100.2, 99.6 (C_5Me$_5$), 10.33, 10.27 (C$_5$*Me*$_5$). Anal. Calcd for $C_{30}H_{39}NO_5Ru_2S_4W_2$: C, 30.24; H, 3.30; N, 1.18. Found: C, 30.78; H, 3.46; N, 1.25.

Thermal Isomerization of 2a. A benzene-d_6 solution (0.4 mL) of **2a** (0.54 mg, 0.48 μmol) was sealed in a Pyrex NMR tube under vacuum. The solution was heated at 80 °C, and the reaction was monitored by ^{1}H NMR spectroscopy. The signal for **1a** appeared, while that of **2a** disappeared completely after 2 h. The conversion of **2a** to **1a** was ca. 90%, determined by the ^{1}H NMR spectrum.

Thermal Isomerization of 3a. A benzene-d_6/acetonitrile-d_3 (3/1) solution (0.4 mL) of **3a** (0.78 mg, 0.93 μmol) was sealed in a Pyrex NMR tube under vacuum. The solution was heated to 80 °C, and the reaction was monitored by ^{1}H NMR spectroscopy. The signal for **5a** appeared, while that for **3a** decreased. After 2 days, the ^{1}H NMR spectrum showed ca. 40% conversion of **3a** to **5a** with 2% recovery of **3a**.

Photochemical Isomerization of 1a. A benzene-d_6 solution (0.4 mL) of **1a** (0.50 mg, 0.44 μmol) was sealed in a Pyrex NMR tube under vacuum. The solution was irradiated with a medium-pressure mercury lamp at 13 °C. After 1 h, the ^{1}H NMR signal of **1a** disappeared completely and formation of **2a** was confirmed. Some unidentified brown precipitates deposited. The conversion of **1a** to **2a** was ca. 50%.

Photochemical Reaction of 5a. A benzene-d_6 solution (0.4 mL) of **5a** (0.42 mg, 0.50 μmol) was sealed in a Pyrex NMR tube under vacuum. The solution was irradiated with a medium-pressure mercury lamp at 13 °C. After 12 h, the signal of **5a** disappeared completely, and several unassignable signals were observed on the ^{1}H NMR spectrum.

Cross-Reaction of [Cp*$_2$Ru$_2$S$_4$] and [(C$_5$Me$_4$Et)$_2$Ru$_2$S$_4$] with [W(CO)$_3$(NCMe)$_3$]. To an acetonitrile solution of [W(CO)$_3$(NCMe)$_3$], which was prepared by refluxing an acetonitrile (4 mL) solution of [W(CO)$_6$] (85 mg, 0.24 mmol), was added a toluene (12 mL) solution of [Cp*$_2$Ru$_2$S$_4$] (35 mg, 0.058 mmol) and [(C$_5$Me$_4$Et)$_2$Ru$_2$S$_4$] (36 mg, 0.058 mmol). The solution was heated at 50 °C for 40 min. After the resulting solution was cooled, volatiles were removed under reduced pressure. The residue was extracted with a toluene/hexane (1/1) mixture (10 mL), and the extract was subjected to silica gel flash column chromatography. Four reddish brown bands were collected with a toluene/hexane (1/1) mixture as an eluent. The evaporation of solvents afforded **1b** (32 mg, 47%), **1a** (26 mg, 40%), **2b** (9 mg, 14%), and **2a** (6 mg, 10%), respectively. Further elution afforded a yellow band containing a mixture of **5a** and **5b** in the molar ratio of 1:1 (1 mg, 1% each).

X-ray Crystallography. Single crystals of all clusters were grown from dichloromethane−hexane solutions at −30 °C. Crystallographic data are summarized in Table 8. The crystals were mounted on glass fibers. Diffraction measurements were carried out on a Rigaku AFC-6S diffractometer using graphite-monochromated Mo Kα radiation (λ = 0.710 73 Å). All reflections were corrected for Lorentz−polarization and absorption effects. Absorption corrections were made by the ψ-scan method; maximum and minimum transmission factors are shown in Table 8. Decay correction was made for **2a**·$2CH_2Cl_2$ and **4**·$2CH_2Cl_2$. Lattice parameters were determined from 24 or 25 reflections with 2θ angles in the range 20−30°. The space groups were identified on the basis of systematic absences and confirmed by successfully solving the crystal structures. Structures were solved by Patterson methods (PATTY) and refined by the least-squares technique. Anisotropic thermal parameters were introduced for all non-hydrogen atoms, except

---

[19] The spectral data suggest that the solid contains an isomer of **7** which is assigned to [{Cp*Ru(CO)}$_2${W(μ_3-S)$_2$(μ-S)$_2$}{*mer*-W(CO)$_3$(CN^{t}Bu)}]: MS (FAB, Xe, *m*-nitrobenzyl alcohol matrix) m/z 1193 (9, M$^+$), 1165 (18, M$^+$ − CO), 1137 (11, M$^+$ − 2CO), 1109 (100, M$^+$ − 3CO); ^{1}H NMR (C_6D_6) δ 1.76 (s, 15H, Cp*), 1.60 (s, 15H, Cp*), 1.06 (s, 9H, ^{t}Bu).

for carbon atoms of dichloromethane in **4**·$2CH_2Cl_2$, which were fixed with isotropic thermal factors. Hydrogen atoms were not located. Data reduction and refinement were performed using teXsan software packages. Selected interatomic distances and bond angles for compounds **1a**, **2a**, **3a**, **4**, **5b**, and **7** are listed in Tables 1−6, respectively.

Supporting Information Available: Text and tables giving X-ray crystallographic data for the crystals **1a**, **2a**·$2CH_2Cl_2$, **3a**, **4**·$2CH_2Cl_2$, **5b**, and **7**. This material is available free of charge via the Internet at http://pubs.acs.org.

OM990432M